Geomechanics and Engineering, *Vol. 17, No. 4 (2019) 405-411*
DOI: https://doi.org/10.12989/gae.2019.17.4.405

Mechanistic representation of the grading-dependent aggregates resiliency using stress transmission column

Yifei Sun[1a], Zhongtao Wang*[2] and Yufeng Gao[1b]

[1]Key Laboratory of Ministry of Education for Geomechanics and Embankment Engineering, College of Civil and Transportation Engineering, Hohai University, Nanjing 210098, China
[2]State Key Laboratory of Coastal and Offshore Engineering, Dalian University of Technology, Dalian 116024, China

(Received July 20, 2017, Revised January 17, 2019, Accepted March 8, 2019)

Abstract. A significant influence of the particle size distribution on the resilient behaviour of granular aggregates was usually observed in laboratory tests. However, the mechanisms underlying this phenomenon were rarely reached. In this study, a mechanistic model considering particle breakage is proposed. It is found to be the combined effects of the coefficient of uniformity and the size range between maximum and minimum particle sizes that influences the resilient modulus of granular aggregates. The resilient modulus is found to undergo reduction with evolution of particle breakage by shifting the initial particle size distribution to a broader one.

Keywords: fractional plastic flow rule; 3d stress state; transformed stress; state dependence

1. Introduction

The resilient behaviour of granular aggregates is a critical issue, especially for public facilities constructed using granular aggregates (Guliyev 2018, Kian *et al.* 2018, Oztoprak *et al.* 2018, Sonmezer *et al.* 2018). For example, high speed rail tracks where a sufficiently high stiffness of the ballast aggregates is usually needed to tolerate the high frequency vibration (Nimbalkar *et al.* 2012, Sevi and Ge 2012, Nimbalkar and Indraratna 2016, Tang *et al.* 2018) induced by the track. To provide instructions for the design and construction of aggregates layer, many laboratory and numerical studies on granular aggregates with different particle size distributions (PSDs) were carried out (Anderson and Fair 2008, Sun *et al.* 2014a, Indraratna *et al.* 2016, McDowell and Li 2016, Park *et al.*, 2018). It was found that the resilient modulus (M_r) of granular aggregates decreased with the increase of coefficient of uniformity (C_u) (Cunningham *et al.* 2013, Yang and Gu 2013, Sun 2017). However, the effect of particle size alone on the resilient behaviour of granular aggregates was unclear. For instances, Sevi and Ge (2012) reported a higher M_r in larger sized aggregates while Suits *et al.* (2009) and Sun (2017) found an increasing M_r with the decreasing particle size. In addition, influence of particle size on the shear modulus was found to be negligible when the median particle size (d_{50}) was varied in a specific range of size (Wichtmann and Triantafyllidis 2009). An alternative insight into the effect of PSD on the resilient behaviour of granular aggregates was attempted based on a micromechanical approach and it was found that soil resiliency was independent on particle size (Yang and Gu 2013). However, this finding was based on monodisperse aggregates representing a uniformly graded granular soil. The force chains in a monodisperse material is rather equally distributed when compared to a polydisperse material (Wichtmann and Triantafyllidis, 2009). The complexity of the effect of particle size or PSD on the aggregates resiliency can be, at least partly, attributed to the variation of the internal stress distribution provided by the different spatial, size and shape distributions of the internal aggregates. In fact, different types of PSDs (including uniform, non-uniform PSDs) were used by researchers in the past. The particle size, shape as well as packing arrangement may vary widely (Sun *et al.* 2014b), which should more or less result in the discrepancy of the above conclusions. Therefore, the role of non-uniformity should be considered appropriately when studying the effect of PSD on the resiliency of granular aggregates.

In this study, an attempt is made to explore the mechanisms underlying the effect of PSD on the resilient behaviour of granular aggregates under elastic shakedown stage. A mechanistic representation considering particle breakage is derived by following a modified parallel-column model developed systematically by Liang and Li (2014). The proposed approach is quantitatively validated by comparing the triaxial test results reported in Sun (2017) and the corresponding theoretical predictions. As demonstrated later, the resilient modulus does remain size independent in specimens with uniform PSDs. However, it varies significantly when the maximum particle size (d_M) starts to depart from the minimum particle size (d_m).

*Corresponding author, Professor
E-mail: zhongtao@dlut.edu.cn
[a]Associate Professor
E-mail: sunny@hhu.edu.cn
[b]Professor
E-mail: yfgao66@163.com

2. Mechanistic representation of PSD-dependence

According to Liang and Li (2014), stress is usually

ISSN: 2005-307X (Print), 2092-6219 (Online)

considered to propagate through the column-like force chains formed by the discrete particles within the specimen (Radjai *et al.* 1998). The varied interaction of the discrete particles in column causes the different resilient responses of granular aggregates with different PSDs. Following Liang and Li (2014), the M_r of a parallel-column is the sum of all particle columns extending the height of the specimen. As the number of particles is large enough in a given triaxial specimen, the height of the column can be obtained by using the probability of occurrence of aggregates with (diametrical) size (d) within the specimen

$$L = \int_{d_m}^{d_M} N d p(d)\, \delta d \tag{1}$$

where N is the number of particles within the specimen; the subscripts m and M indicate the minimum and maximum particles within the sample. $p(d)$ is the density distribution function of particles with size (d) and can be formulated as (Einav 2007)

$$p(d) = \frac{(3-\alpha)d^{2-\alpha_0}}{d_M^{3-\alpha_0} - d_m^{3-\alpha_0}} \tag{2}$$

where α_0 is a material parameter and equal to the fractal dimension only if ballast particles are completely crushed to the ultimate fractal PSD. It should be noted that particle columns in real granular materials are rarely cylindric. However, this assumption bears the simplicity and yet efficient in modelling the resilient stress and strain behaviour of granular samples. Therefore, Eq. (1) is used to explain the laboratory observation of ballast subjected to triaxial loads. For triaxial specimens subjected to compressive loads, resilient deformation is attributed to the movements of particles in the stress-carrying column. According to the law of elasticity, the normal contact stiffness ($k_{i-1,i}^n$) between two adjacent particles can be expressed as

$$\frac{1}{k_{i-1,i}^n} = \frac{1}{E}\left(\frac{1}{d_{i-1}} + \frac{1}{d_i}\right) \tag{3}$$

where E is the characteristic modulus of the material. Hence, the stiffness of the whole stress-carrying column (K) is

$$\frac{1}{K} = \frac{1}{E}\left[\int_{d_m}^{d_{N-1}} (N-1)d^{-1}p(d)\delta d + \int_{d_2}^{d_M} (N-1)d^{-1}p(d)\delta d\right] \tag{4}$$

where $d_{N\text{-}1}$ and d_2 are the second large and small particle diameters, respectively, within the specimen. As N is large enough in the triaxial element, $N - 1 \approx N$, $d_{N\text{-}1} \approx d_N = d_M$ and $d_2 \approx d_1 = d_m$. Therefore, Eq. (4) can be approximately expressed as

$$\frac{1}{K} = \frac{2}{E} N \int_{d_m}^{d_M} d^{-1}p(d)\delta d \tag{5}$$

Further substituting Eq. (1) into Eq. (5), yields

$$K = \frac{E}{2L}\frac{\int_{d_m}^{d_M} dp(d)\delta d}{\int_{d_m}^{d_M} d^{-1}p(d)\delta d} \tag{6}$$

The overall stiffness of the triaxial specimen can be obtained by summing the stiffness of all the parallel stress-carrying columns as

$$K_t = mK = \frac{\frac{D^2}{2}E}{L(1+e)}\frac{\langle d\rangle}{\langle d^2\rangle\langle d^{-1}\rangle} \tag{7}$$

where m is the number of parallel columns and can be expressed as

$$m \approx \frac{\frac{\pi D^2}{4}}{(1+e)\int_{d_m}^{d_M} \frac{\pi d^2}{4} p(d)\delta d} \tag{8}$$

where D is the diameter of the triaxial specimen, e is the current void ratio that can be expressed as (Åberg 1992)

$$e = 2c\frac{\int_0^1 [F(d)/d]\delta F(d)}{\int_0^1 [1/d]\delta F(d)} + 2t \tag{9}$$

where c is a shape parameter, depending on the shape of particles ($c \approx 0.6$ for spheres, $c \approx 0.75$ for sand and gravel, and $c \approx 1.0$ for crushed rock); t is a densification parameter, depending on the degree of densification ($t \approx 0.18$ for loosest packing, and $t \approx 0$ for densest packing). In this study, $c \approx 1.0$ and $t \approx 0$ are used for all specimens. $F(d)$ is the cumulative distribution function for a given PSD and is formulated as

$$F(d) = \int_{d_m}^{d} p(d)\delta d \tag{10}$$

There are three additional functions in Eq. (10), i.e.,

$$\langle d\rangle = \int_{d_m}^{d_M} dp(d)\delta d \tag{11}$$

$$\langle d^2\rangle = \int_{d_m}^{d_M} d^2 p(d)\delta d \tag{12}$$

$$\langle d^{-1}\rangle = \int_{d_m}^{d_M} d^{-1} p(d)\delta d \tag{13}$$

As the current density distribution function $p(d)$ can be related to the initial and fractal density distribution function of the material, the following relationship can be obtained by following Einav (2007)

$$p(d) = (1-B)p_0(d) + Bp_u(d) \tag{14}$$

where B is the fractal breakage ratio defined by Einav (2007). The use of B instead of other indices is for the purpose of theoretical analysis. During loading, granular aggregates would break which could change the initial grading of the aggregates. The incorporation of B is to capture this change. $p_0(d)$ is the initial density distribution function with the minimum particle size equal to d_{m0}; $p_u(d)$ is the fractal density distribution function and can be given as

$$p_u(d) = \frac{(3-\alpha)d^{2-\alpha}}{d_M^{3-\alpha} - d_{mf}^{3-\alpha}} \tag{15}$$

where α is the fractal dimension and can be set as 2.6 (Coop *et al.* 2004, Einav 2007, Xiao *et al.* 2014). d_{mf} is equal to

0.074 mm, which is the minimum size counted for granular soils (ASTM 2006). By substituting Eq. (14) into Eqs. (11) – (13), the following relations can be obtained

$$\langle d \rangle = (1-B)\langle d \rangle_0 + \langle d \rangle_u \tag{16}$$

$$\langle d^2 \rangle = (1-B)\langle d^2 \rangle_0 + \langle d^2 \rangle_u \tag{17}$$

$$\langle d^{-1} \rangle = (1-B)\langle d^{-1} \rangle_0 + \langle d^{-1} \rangle_u \tag{18}$$

where

$$\langle d^j \rangle_0 = \int_{d_{m0}}^{d_M} d^j p_0(d)\delta d \, , j = -1{,}1{,}2 \tag{19}$$

$$\langle d^j \rangle_u = \int_{d_m}^{d_M} d^j p_u(d)\delta d \, , j = -1{,}1{,}2 \tag{20}$$

The physical meanings of Eqs. (16) – (18) can be found in Sun *et al.* (2018). Eq. (16) denotes the average particle size while Eq. (17) denotes the distribution pattern of particle sizes around $\langle d \rangle$. Eq. (18) indicates the harmonic mean of particle sizes, describing the size contribution of each particle. As can be observed, the overall stiffness is highly dependent on not only the scales of the sample but also the PSD and particle breakage. A similar result can be found in an elastic continuum that is increasingly easier to bend when the length to width ratio increases. Furthermore, the M_r of a triaxial specimen can be determined by

$$M_r = \frac{\sigma}{\varepsilon_r} = \frac{P/(\frac{\pi D^2}{4})}{U/L} = \frac{P}{U}\frac{4L}{\pi D^2} \tag{21}$$

where σ and ε_r are the stress and recoverable strain, respectively; P and U are the external force and displacement of the specimen. According to Newton's law, $P = K_t U$. Then, further substituting Eq. (7) into Eq. (14), the final formula of the resilient modulus can be given as

$$M_r = \frac{2E}{\pi(1+e)} \frac{\langle d \rangle}{\langle d^2 \rangle \langle d^{-1} \rangle} \tag{22}$$

Moreover, as Eq. (22) does not consider the effect of particle arrangement, such as sliding and rotation, a coefficient H similar to Liang and Li (2014) is therefore introduced

$$M_r \propto H \frac{2E}{\pi(1+e_f)} g(d,B) \tag{23}$$

where e_f is the void ratio at final state. Based on DEM simulation (Liang and Li 2014), H had been shown to be well correlated by the simulated results. A linear variation of H with the contact density which represented the interaction between aggregates had been found. Therefore, H can approximately capture the interactions between aggregates. Function $g(d, B)$ reflects the influences of PSD and breakage that can be formulated as

$$g(d,B) = \frac{\langle d \rangle_0 (1-B) + \langle d \rangle_u B}{\langle d^2 \rangle_0 (1-B) + \langle d^2 \rangle_u B} \frac{1}{\langle d^{-1} \rangle_0 (1-B) + \langle d^{-1} \rangle_u B} \tag{24}$$

$g(d, B)$ is a measure of how the initial PSD evolves to the ultimate PSD. It is noted that the pressure dependence of stiffness is not considered in Eqs. (22) and (23) for simplicity. However, it can be incorporated by using pressure-dependent E. For more details, one can referrer to Sun *et al.* (2018). Moreover, Eq. (24) assumes that granular soil is homogenous and should break towards a fractal grading, which is supported by many studies (Coop *et al.* 2004, Einav 2007).

3. Discussions

It is found from Eq. (23) that M_r is in direct proportion to $g(d,B)/(1+e)$, given that all the samples were tested under the same conditions. To validate the proposed approach, a series of large-scale triaxial test results reported by Indraratna *et al.* (2016) and Sun (2017) are used in this study. The physical properties of ballast aggregates and the relevant test program can be found in Table 1. For more details of the test material and test setup, one can refer to Sun (2017), where grading variations during the whole testing procedures were also given. Fig. 1 shows the initial and final gradings of each test.

Fig. 2 shows the relationship between the experimental results of the M_r in (Sun 2017) and the corresponding calculated values of the function $g(d,B)/(1+e_f)$ at the end of each cyclic test. In general, M_r increases with the increase of $g(d,B)/(1+e_f)$, which verifies the rationality of Eq. (23).

Table 1 Physical properties and test program of ballast specimens

PSD No.	e_0	C_u	d_M (mm)	d_{50} (mm)	d_m (mm)	σ_3' (kPa)	q_{min} (kPa)	q_{max} (kPa)	B		e_f	
									20Hz	30Hz	20Hz	30Hz
1	0.78	1.2	53	49.4	2.36	30	45	230	0.031	0.048	0.70	0.61
2	0.75	2.0	53	40.4	2.36				0.024	0.046	0.68	0.64
3	0.75	3.0	53	34.2	2.36				0.040	0.076	0.62	0.53
4	0.75	1.9	53	40.8	9.5				0.035	0.052	0.69	0.61
5	0.75	1.9	40	30.5	9.5				0.019	0.067	0.70	0.64
6	0.75	1.9	31.5	22.7	9.5				0.024	0.068	0.72	0.68

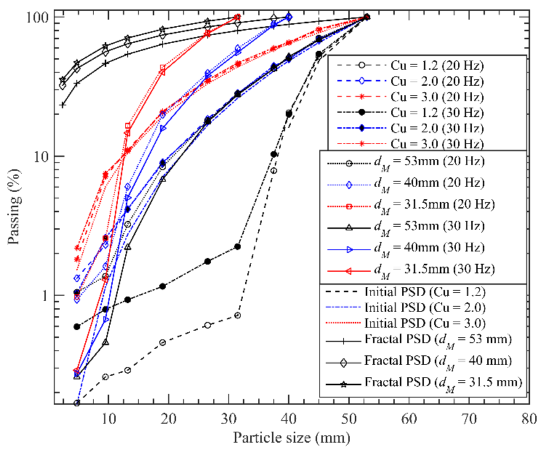

Fig. 1 Initial, final and fractal gradings

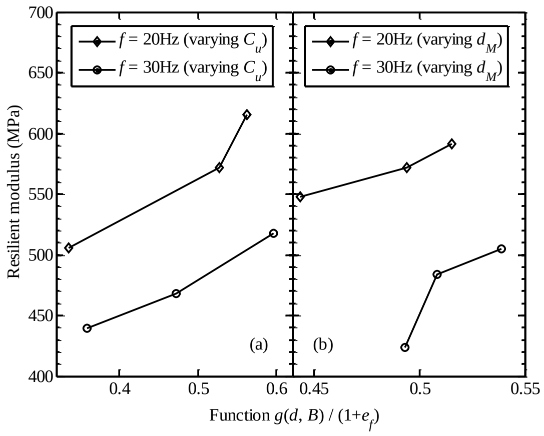

Fig. 2 Variation of resilient modulus with function $g(d, B)$ / $(1+e_f)$ at the end of each test

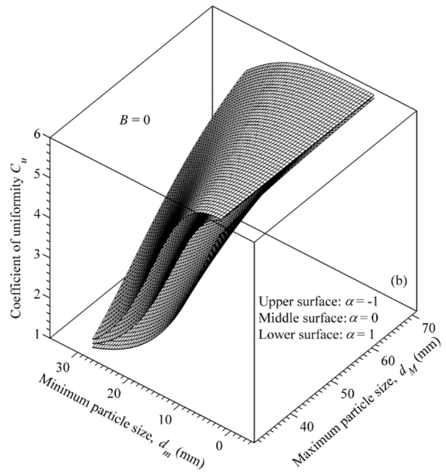

Fig. 4 Variation of C_u with particle size

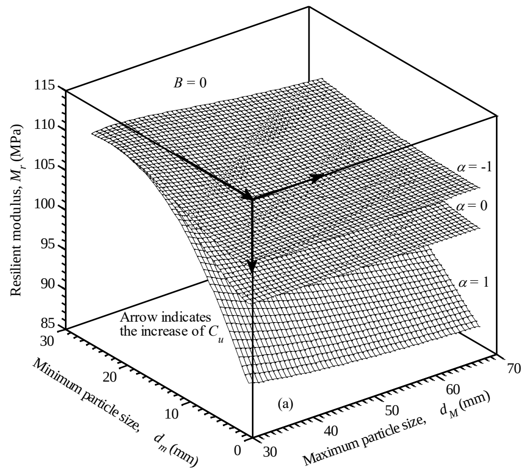

Fig. 3 Effect of the PSD on the resilient modulus

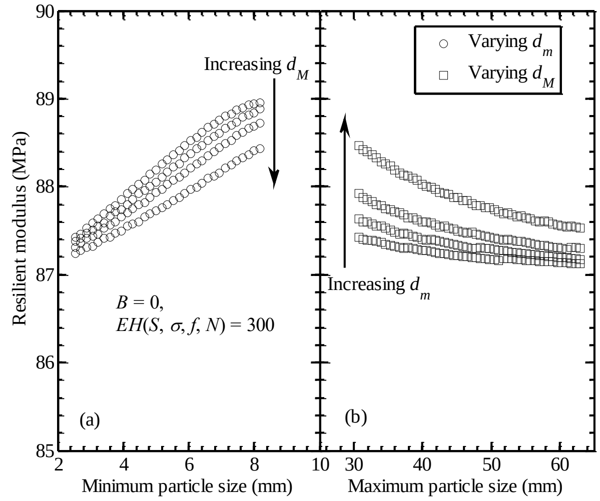

Fig. 5 Mechanistic representation of the evolution of resilient modulus with (a) varying d_m and (b) varying d_M at constant C_u

The influence of the PSD on the M_r of ballast can be further represented by using Eq. (23), as shown in Figs. 3 and 4. It is noted that Figs. 3 and 4 does not consider particle breakage. The effect of breakage on material resilience will be discussed later. Fig. 3 presents the evolution of M_r with the varying exponent α and particle size. Note that the exponent α remains constant on a given surface but changes from one surface to another. An increase in α will result in the increase of C_u (Fig. 4) which further reduces the M_r of granular aggregates as shown in Fig. 3. For soils with the fixed d_M and α, M_r is also observed to increase with increasing d_m. However, if the aggregates were initially in a uniform grading as shown in Fig. 3 with $\alpha = -1$, d_m do not have significant influence on M_r until a substantial large value is reached. Because smaller aggregates mainly lay within the voids among larger sized aggregates and cannot effectively transmit forces in uniformly graded aggregates. When the minimum sized aggregates are further replaced by the relatively larger aggregates, i.e., aggregates with sizes approaching the void sizes of the original material, they will start to push apart the larger skeleton aggregates, affecting the subsequent mechanical performance of the aggregates. However, in well graded aggregates, even the minimum sized aggregates play a role in carrying the external applied stress at the right beginning. Any further updating of the minimum particle size to a higher value will lead to an increase in the material resiliency.

For those with the fixed d_m and α, a decrease in M_r with increasing d_M is observed. The variation of particle size implicitly causes the change of C_u (Fig. 4) and the relative particle configuration which consequently results in the change of M_r as shown in Fig. 3. At the particle level, the material resiliency is highly dependent on the magnitude and distribution of contact normal forces. With increasing d_m or decreasing d_M, the magnitude and distribution of contact normal forces become more uniform, which lead to further increase of resilient modulus in addition to that caused by increasing coordination number (Yang and Gu 2013). This is in agreement with the experimental results of granular aggregates from available literatures (Hardin and Kalinski 2005, Wichtmann and Triantafyllidis 2009, Sun, 2017). Moreover, the highest M_r is found to be in those aggregates with almost the same d_M and d_m. A constant M_r can also be anticipated from Eq. (23) for the uniformly graded aggregates (d_m = d_M) under the same testing condition. This actually conforms to the experimental

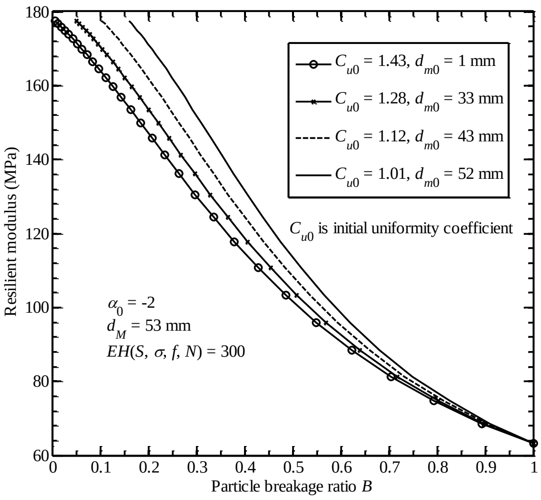

Fig. 4 Variation of C_u with particle size

results by Yang and Gu (2013), where an almost constant elastic modulus was reported for granular soils with nearly uniform PSDs.

Fig. 5 presents the mechanical representation of the influences of d_m (Fig. 5(a)) and d_M (Fig. 5(b)) on the resilient modulus of specimens with a constant value of C_u (= 1.9). As shown in Fig. 5(a), the increase of d_m causes a slight increase in M_r, where a higher increasing rate is also observed for samples with an initially lower d_M. However, the increase of d_M is shown to decrease the M_r, where a higher decreasing rate is observed for samples with an initially higher d_m. This is in accordance with the test results as reported in Fig. 2. Therefore, it is the combined effects of the deviation from d_m to d_M and C_u that influence the elastic behaviour of granular aggregates. It is noted that a typical fixed value of B or EH is used for interpretation in Fig. 5. The effect of varying B is not presented here for clarity. As EH is a multiplier, it only influences the value but not the evolution trend shown in Fig. 5.

In addition to the effect of PSD, particle breakage also shows a great influence on the mechanical response of granular aggregates (Wu *et al.* 2018). As shown in Fig. 6, M_r decreases significantly with the increase of the particle breakage ratio B. Although initially different resilient moduli are expected in the different PSDs, they are observed to approach the same value when the initial PSDs shift towards the ultimate fractal PSD where B = 1. This is because the ultimate fractal PSD remains the same for soils with the same initial d_M according to the particle breakage theory proposed by Einav (2007), where an equivalent final particle configuration can be expected. The reason for using constant EH (= 300) is the same as that discussed for Fig. 5 and thus not repeated here for simplicity.

4. Conclusions

Dependence of the resilient modulus on the PSD of granular aggregates was investigated in this paper via mechanical representation. The main findings are summarised as follows:

(1) An expression for evaluating the resilient modulus of granular aggregates with different PSDs was proposed by employing a modified parallel-column model. All the derivations and discussions were based on parallel-column model, which was not usually observed in laboratory testing. However, to consider this deficiency, a modified constant was used as suggested by Liang and Li (2014). The proposed expression was then validated by using the large-scale triaxial test results of ballast aggregates from available literature.

(2) It was found that the combined effects of the size span between the maximum and minimum particle sizes as well as the coefficient of uniformity that influenced the resilient modulus of granular aggregates. The highest resilient modulus was found to be in the uniform graded samples having a narrow range between the minimum and maximum particle sizes. Any decrease of the minimum particle size or increase of the maximum particle size would result in a significantly reduced resilient modulus.

(3) A constant resilient modulus was expected for granular aggregates with any type of uniform PSD given the same testing condition.

(4) Apart from the PSD, particle breakage can be also regarded as a critical factor that influences the resiliency of granular aggregates. More serious breakage would result in a lower resilient modulus.

(5) This study did not consider the shape variation and the associated sliding and rotation of the granular aggregates. All the derivations were based on pseudo-static assumption where the Newton's law of dynamic motion along the normal contact direction was taken into account. Therefore, further studies should be carried out to model the real configuration of the granular aggregates under randomly dynamic motion.:

Acknowledgements

The financial supports provided by the National Natural Science Foundation of China (Grant Nos. 41630638, 51679068), the National Key Basic Research Program of China ("973" Program) (Grant No. 2015CB057901), the Fundamental Research Funds for the Central Universities (Grant No. 2017B05214) and the Project funded by China Postdoctoral Science Foundation (Grant No. 2017M621607) are greatly appreciated.

References

Åberg, B. (1992), "Void ratio of noncohesive soils and similar materials", *J. Geotech. Eng.*, **118**(9), 1315-1334.

Anderson, W.F. and Fair, P. (2008), "Behavior of railroad ballast under monotonic and cyclic loading", *J. Geotech. Geoenviron. Eng.*, **134**(3), 316-327.

ASTM (2006), *Standard Test Method for Sieve Analysis of Fine and Coarse Aggregates*, ASTM International, West Conshohocken, Pennsylvania, U.S.A.

Coop, M., Sorensen, K., Freitas, T.B. and Georgoutsos, G. (2004), "Particle breakage during shearing of a carbonate sand", *Géotechnique*, **54**(3), 157-163.

Cunningham, C.N., Evans, T.M. and Tayebali, A.A. (2013), "Gradation effects on the mechanical response of crushed stone aggregate", *Int. J. Pavement Eng.*, **14**(3), 231-241.

Einav, I. (2007), "Breakage mechanics—Part I: Theory", *J. Mech. Phys. Solids*, **55**(6), 1274-1297.
Guliyev, H.H. (2018), "Geomechanical analysis of elastic parameters of the solid core of the Earth", *Geomech. Eng.*, **14**(1), 19-27.
Hardin, B.O. and Kalinski, M.E. (2005), "Estimating the shear modulus of gravelly soils", *J. Geotech. Geoenviron. Eng.*, **131**(7), 867-875.
Indraratna, B., Sun, Y. and Nimbalkar, S. (2016), "Laboratory assessment of the role of particle size distribution on the deformation and degradation of ballast under cyclic loading", *J. Geotech. Geoenviron. Eng.*, **142**(7), 04016016.
Kian, A.R.T., Zakeri, J.A., and Sadeghi, J. (2018), "Experimental investigation of effects of sand contamination on strain modulus of railway ballast", *Geomech. Eng.*, **14**(6), 563-570.
Liang, Y. and Li, X. (2014), "An expression for the stiffness coefficient of a rectangular sample of granular material with random packing structure", *Granul. Matter*, **16**(4), 583-595.
McDowell, G.R. and Li, H. (2016), "Discrete element modelling of scaled railway ballast under triaxial conditions", *Granul. Matter*, **18**(3), 1-10.
Nimbalkar, S. and Indraratna, B. (2016), "Improved performance of ballasted rail track using geosynthetics and rubber shockmat", *J. Geotech. Geoenviron. Eng.*, **142**(8), 04016031.
Nimbalkar, S., Indraratna, B., Dash, S.K. and Christie, D. (2012), "Improved performance of railway ballast under impact loads using shock mats", *J. Geotech. Geoenviron. Eng.*, **138**(3), 281-294.
Oztoprak, S., Sargin, S., Uyar, H.K. and Bozbey, I. (2018), "Modeling of pressuremeter tests to characterize the sands", *Geomech. Eng.*, **14**(6), 509-517.
Park, T., Kim, H., Tanvir, M., Lee, J. and Moon, S. (2018), "Influence of coarse particles on the physical properties and quick undrained shear strength of fine-grained soils", *Geomech. Eng.*, **14**(1), 99-105.
Radjai, F., Wolf, D.E., Jean, M. and Moreau, J.J. (1998), "Bimodal character of stress transmission in granular packings", *Phys. Rev. Lett.*, **80**(1), 61-64.
Sevi, A. and Ge, L. (2012), "Cyclic behaviors of railroad ballast within the parallel gradation scaling framework", *J. Mater. Civ. Eng.*, **24**(7), 797-804.
Sonmezer, Y.B., Bas, S., Isik, N.S. and Akbas, S.O. (2018), "Linear and nonlinear site response analyses to determine dynamic soil properties of Kirikkale", *Geomech. Eng.*, **16**(4), 435-448.
Suits, L.D., Sheahan, T.C., Patel, A., Bartake, P.P. and Singh, D.N. (2009), "An empirical relationship for determining shear wave velocity in granular materials accounting for grain morphology", *Geotech. Test. J.*, **32**(1), 1-10.
Sun, Q.D., Indraratna, B. and Nimbalkar, S. (2014a), "Effect of cyclic loading frequency on the permanent deformation and degradation of railway ballast", *Géotechnique*, 746-751.
Sun, Y. (2017), "Effect of particle angularity and size distribution on the deformation and degradation of ballast under cyclic loading", Ph.D., University of Wollongong, Wollongong, Australia.
Sun, Y., Indraratna, B. and Nimbalkar, S. (2014b), "Three-dimensional characterisation of particle size and shape for ballast", *Geotech. Lett.*, **4**(3), 197-202.
Sun, Y., Shen, Y. and Chen, C. (2018), "A grading parameter for evaluating the grading-dependence of the shear stiffness of granular aggregates", *Particuology*, **36**, 193-198.
Tang, L.S., Chen, H.K., Sun, Y.L., Zhang, Q.H. and Liao, H.R. (2018), "Traffic-load-induced dynamic stress accumulation in subgrade and subsoil using small scale model tests", *Geomech. Eng.*, **16**(2), 113-124.
Wichtmann, T. and Triantafyllidis, T. (2009), "Influence of the grain-size distribution curve of quartz sand on the small strain shear modulus Gmax", *J. Geotech. Geoenviron. Eng.*, **135**(10), 1404-1418.
Wu, Y., Hyodo, M. and Aramaki, M. (2018), "Undrained cyclic shear characteristics and crushing behaviour of silica sand", *Geomech. Eng.*, **14**(1), 1-8.
Xiao, Y., Liu, H., Chen, Y. and Jiang, J. (2014), "Strength and deformation of rockfill material based on large-scale triaxial compression tests. II: Influence of particle breakage", *J. Geotech. Geoenviron. Eng.*, **140**(12), 04014071.
Yang, J. and Gu, X.Q. (2013), "Shear stiffness of granular material at small strains: does it depend on grain size?", *Géotechnique*, **63**(2), 165-179.

CC

Notations

B	Einav's breakage index
C_u	coefficient of uniformity
C_{u0}	coefficient of uniformity of the initial grading
c	shape parameter
D	diameter of the tested sample
d	particle size
d_i	particle size of i^{th} particle
d_M	maximum particle size
d_m	minimum particle size
d_{m0}	minimum particle size before test
d_{mf}	minimum particle size counted for granular soils
d_{50}	median particle size
E	characteristic modulus of the particle
e	void ratio
e_0	initial void ratio
e_f	final void ratio
$F(d)$	cumulative distribution function for a given grading
f	cyclic loading frequency
K	stiffness of a particle column
K_t	stiffness of all the particle columns
$k^n_{i-1,i}$	normal contact stiffness between i^{th} and i-1^{th} particles

PSD	particle size distribution
P	external force of the specimen
$p(d)$	current density distribution function
$p_0(d)$	initial density distribution function
$p_u(d)$	ultimate density distribution function
q_{min}	minimum deviator stress
q_{max}	maximum deviator stress
t	densification parameter
L	length of the particle column
M_r	resilient modulus
U	displacement of the specimen
α_0	initial fractal dimension
α	ultimate fractal dimension
σ'_3	confining pressure
ε_r	recoverable strain